Separation and Purification Technology 237 (2020) 116377

Contents lists available at ScienceDirect

Separation and Purification Technology

journal homepage: www.elsevier.com/locate/seppur

Fabrication of bead-on-string polyacrylonitrile nanofibrous air filters with superior filtration efficiency and ultralow pressure drop

Jinhui Jeanne Huang[a], Yuxiao Tian[a], Rong Wang[b,c], Miao Tian[d], Yuan Liao[a,*]

[a] Sino-Canadian Joint R&D Center for Water and Environmental Safety, College of Environmental Science and Engineering, Nankai University, No.38 Tongyan Road, Jinnan District, Tianjin 300350, PR China

[b] Singapore Membrane Technology Centre, Nanyang Environment and Water Research Institute, Nanyang Technological University, 1 Cleantech Loop, Singapore 637141, Singapore

[c] School of Civil and Environmental Engineering, Nanyang Technological University, 50 Nanyang Avenue, Singapore 639798, Singapore

[d] Center for Ecological and Environmental Sciences, Northwestern Polytechnical University, Xi'an 710072, China

ARTICLE INFO

Keywords:
Bead-on-string
Air filter
Solid aerosol
Oil aerosol
Electrospinning

ABSTRACT

The presence of ultrafine particle matter (PM) in air is one of the most hazardous environmental issues because of their severe threat to human health. Design and development of cost-effective and energy-efficient air filters to remove the PM by facile methods are highly demanded. Electrospun nanofibrous membranes have been explored for PM filtrations as they can achieve high removal efficiencies due to their ultrafine nanofibers. However, their enhanced particle removal efficiencies are at the cost of high pressure drops. In this work, porous bead-on-string filters with nanobeads along the nanofiber axis have been successfully fabricated by optimizing the polyacrylonitrile (PAN) concentration of electrospun dopes and ambient humidity condition during the electrospinning process. The combined effects of polymer concentration and humidity condition could achieve an unbalanced status between the repulsive and constrictive forces along the jets from the spinneret in the electrospinning process, which generated a filter with a desirable bead-on-string morphology. The nanobeads are able to reduce the packing density and alleviate the pressure drop through the filter while the ultrafine nanofibers guarantee the PM removal efficiency. Besides, the effects of nanofiber diameter, airflow rate and nanobead density on the filtration efficiency and pressure drop of NaCl solid and Paraffin oil aerosols with an average diameter of 300 nm have been investigated systematically. With the assistance of bead-on-string construction, the pristine PAN filter can easily achieve an excellent efficiency above 99% with a low pressure drop of 27 Pa at an airflow rate of 4.2 cm/s. This work suggests that transformation of electrospun filters from a nanofibrous structure to a bead-on-string morphology *via* the adjustments of polymer concentration and ambient humidity is sufficient to generate filter mediums with excellent efficiency and low airflow resistance for air filtration applications, which is also facile to be scaled up as no special equipment and costly chemicals are required.

1. Introduction

Severe air pollution due to rapid developments of industrialization and urbanization is one of the top environmental concerns in both developing and developed countries [1]. Many epidemiological and toxicological studies have demonstrated that the deteriorative air quality has negative impacts on human health, which may result in mental disorder, morbidity and disability [2]. Ultrafine particulate matter (PM) is one of the most hazardous environmental issues and main component of fog and haze [3]. These fine particles show longer residence time and larger surface area carrying other pollutants, which can easily lodge into respiratory system via inhalation and result in cardiovascular and respiratory diseases by dissolving in the blood [2]. The increasing awareness of human health threats due to the ultrafine PM demands effective technologies to mitigate it. The conventional PM removal methods include baghouse filtration, gravity settling, centrifugation, electrostatic separation and fibrous filter filtration [4–6]. Among these technologies, the fibrous filters have attracted increasing attention in removing ultrafine PM and been applied in a great number of air filtration application, attributed to their high efficiency and economic benefits [7–9]. In contrast to the microsized fibers with an average diameter from several to ten micrometers, the nanofibrous air filters with an average diameter below 1.0 μm exhibit a higher removal efficiency towards ultrafine PM, especially for those particles with an

* Corresponding author.
E-mail address: liaoyuan@nankai.edu.cn (Y. Liao).

https://doi.org/10.1016/j.seppur.2019.116377
Received 11 August 2019; Received in revised form 22 November 2019; Accepted 1 December 2019
Available online 04 December 2019
1383-5866/

aerodynamic diameter less than 1.0 μm [10,11].

The properties of nanofibrous filters are usually evaluated by the PM removal efficiency and pressure drop, which are calculated according to the particle concentrations and pressure differences of the upstream and downstream through the filter [12]. An excellent air filter should exhibit a high PM removal efficiency and a low pressure drop. It is usually anticipated that the improvement of removal efficiency is at the cost of reduced air permeability due to tightened filter structure and PM deposition on the filter. As a result, plentiful efforts have been devoted to enhance the removal efficiency of a filter without sacrificing air permeability [13–16]. As the removal efficiency of a filter is determined by both intrinsic chemical property and morphology of the nanofiber, it is critical to select an appropriate material as well as establish a suitable structure. Numerous polymers, including polyacrylonitrile (PAN), polyvinyl pyrrolidone (PVP), polyvinyl acetate (PVA), polystyrene (PS), polypropylene (PP) and *etc*, have been electrospun as air filters [17–20]. Among these polymers, the PAN nanofibrous membranes are often used as the filtration mediums due to the excellent chemical and thermal stabilities. Besides, the dipole-dipole and induced-dipole forces of PAN are able to promote the interaction between PMs and nanofibers and achieve the highest PM capture efficiency [17].

In order to further enhance the ultrafine PM removal capacity, various nanofillers such as graphene oxide (GO), reduced graphene oxide (rGO) and metal organic frameworks (MOFs), have been embedded into the electrospun PAN nanofibers [21–23]. The excellent adsorption property of GO could significantly enhance the $PM_{2.5}$ (particle size $<$ 2.5 μm) capture capacity [21]. The rGO nanosheet-embedded PAN nanofibers showed an excellent $PM_{2.5}$ removal efficiency above 99.9% and a pressure drop as low as 70 Pa, which should be due to more $PM_{2.5}$ capture sites from rGO [22]. Besides, four types of MOFs were incorporated into nanofibrous filters with a loading amount up to 60 wt% [24]. The outstanding capture ability of MOFs and strong binding affinity between MOFs and ultrafine PM significantly enhanced their PM removal efficiencies. However, although the hybrid nanofibers have demonstrated their competitive performance, the leakage of these nanofillers as well as high costs of specific nanofillers impede their practical applications.

In addition to the optimization of their intrinsic chemical properties, electrospun composite nanofibrous filters with multilevel structures have been developed to enhance their air filtration properties [25–27]. An anti-deformed poly(ethylene oxide) (PEO)@ PAN/polysulfone (PSU) fibrous filter with a binary structure was fabricated by multi-jet electrospinning and physical bonding [11]. Benefiting from smooth PAN nanofibers, porous PSU microfibers and PEO bonding, the composite membrane possessed a high filtration efficiency above 99%, a low pressure drop of 95 Pa as well as a robust mechanical property. Moreover, a highly integrated PSU/PAN/polyamide-6 (PA-6) filter composing of PSU microfibers with an average diameter of 1 μm, PAN nanofibers with an average diameter of 200 nm and PA-6 nanonets with an average diameter of 20 nm, was capable to impede the penetration of 300 nm aerosols with a high removal efficiency above 99% and a low pressure drop pf 118 Pa [10]. The strategy of constructing a three-dimensional (3D) functional structure with various materials is promising in fabricating efficient air filters. Nonetheless, these multilevel air filters need various materials and complicated fabrication procedures.

In this work, it is the first time that the porous bead-on-string PAN filters were designed and fabricated for ultrafine PM removal by optimizing the PAN concentration of electrospun dopes and ambient humidity. This structure has the potential to achieve a high PM removal efficiency as well as a low pressure drop without usage of highly costed nano-additives, various kinds of materials and tedious fabrication steps. To investigate the effects of nanofibrous and bead-on-string structures on fine PM removal efficiency, a series of nanofibrous and bead-on-string membranes were prepared in this work. The effects of the filter morphologies, nanofiber diameters and airflow rates on removing NaCl solid and Paraffin oil aerosols with an average diameter of 300 nm were examined systematically in this work. The practical application, mechanical robustness and long-term air filtration efficiency of as-developed filter were also evaluated. It is expected that this work can propose a facile method to produce highly effective and low cost air filters for indoor air purification and respiratory protection.

2. Experimental section

2.1. Materials

The polyacrylonitrile (PAN, Mw = 150,000 g mol^{-1}) was supplied by Sigma-Aldrich (USA) as the main polymer. N, N-dimethylformamide (DMF, 99.5%) was purchased from Damao Chemical Co. LTD. (Tianjin, China) as the solvent to prepare electrospun dope solutions. Sodium chloride (NaCl, 99.5%) and Paraffin liquid (99.5%) used in air filtration test were bought from Wuxi Jingke Chemical Co. LTD, Jiangsu, China. The non-woven substrate (thickness 0.1 mm, basic weight 20 g m^{-2}) was purchased from Dongwan Jialianda nonwovens Co. LTD. Guangdong, China.

2.2. Preparation of electrospun PAN air filters

In this work, three PAN dope solutions with different concentrations including 11 wt%, 8 wt% and 5 wt% were prepared to fabricate air filters with various morphologies by electrospinning. The designed amount of PAN was dissolved in DMF by stirring mechanically at 100 ℃ for at least 12 h. The homogeneous and transparent solutions were then degassed and cooled down to room temperature before electrospinning. Prior to electrospinning, a non-woven support without any PM removal efficiency and air flow resistance was pasted on a grounded stainless steel drum collector. It is worth pointing out that the non-woven used in this work has no PM removal efficiency and air flow resistance. Thus, the non-woven support layer should not possess any significant influence on the removal efficiency and air flow resistance of as-developed PAN air filters. The polymer solutions were then loaded into plastic syringes and ejected by a syringe pump. A positive voltage was applied on the metal spinnerets connected with the syringes while a negative voltage was applied on the grounded collector. The distance between the spinnerets and collector was set as 15 cm. The entire electrospinning equipment was placed in a chamber at a constant temperature (20 ± 2 ℃) and variable relative humidity (RH), including 30%, 40%, 50% and 60%. The PAN air filters fabricated by electrospinning the 11 wt% PAN solution at the RH of 30%, 40%, 50% and 60% are nominated as #P11-3, #P11-4, #P11-5 and #P11-6, respectively. Analogously, the filters developed by electrospinning the 8 wt% PAN solution at the RH of 30%, 40%, 50% and 60% are named as #P8-3, #P8-4, #P8-5 and #P8-6, respectively. The filters developed by electrospinning 8 wt% and 5 wt% PAN solutions using two spinnerets simultaneously at the RH of 30%, 40%, 50% and 60% are named as #P8/5-3, #P8/5-4, #P8/5-5 and #P8/5-6, respectively. The detailed electrospun parameters are summarized in Table 1. The basis weights of all the filters are kept as 1.77 g m^{-2}.

2.3. Characterization of electrospun PAN filters

The surface morphologies of PAN membranes were examined by a field emission scanning electroscope (FE-SEM, JSM-7200F, JEOL Asia Pte Ltd., Japan) at an acceleration voltage of 5 kV. The diameter and diameter distribution of nanofibers and nanobeads were measured by Nano Measurer. Each simple was measured at more than 150 positions. The density of beads (DB, mm^{-2}) are calculated by the following equation [28],

$$D_B = N/S \quad (1)$$

where N is the number of nanobeads, S is the area of the membrane

Table 1
Electrospun conditions of the PAN air filters developed in this work.

	Dope Composition (wt %)	Dope Flow Rate (mL h^{-1})	Relative Humidity (%)	Temperature (°C)	Time (min)	Travel Speed (mm min^{-1})	Travel Distance (cm)	Working Distance (cm)	Voltage (kV)	Receiving Speed (m min^{-1})
#P11-3	PAN/DMF = 11/89	0.80	30 ± 2	20 ± 2	11	500	14	15	+12/-4	60
#P11-4			40 ± 2							
#P11-5			50 ± 2							
#P11-6			60 ± 2							
#P8-3	PAN/DMF = 8/92	1.60	30 ± 2	20 ± 2	15	500	14	15	+16/-4	60
#P8-4			40 ± 2							
#P8-5			50 ± 2							
#P8-6			60 ± 2							
#P8/5-3	PAN/DMF = 8/92	1.60	30 ± 2	20 ± 2	9/9	500	14	15	+16/-4	60
#P8/5-4	PAN/DMF = 5/95		40 ± 2							
#P8/5-5			50 ± 2							
#P8/5-6			60 ± 2							

sample (mm^2). The mechanical properties of the membranes were tested through a tensile tester (UTM2202, Shenzhen Suns Technology Stock Co. Ltd., Guangdong, China).

2.4. Evaluation of PM removal efficiencies of the filters

Fig. 1 shows the scheme of automatic PM filtration tester (G506, Shanghai Fanbiao Textile Testing Technology Co. Ltd., Shanghai, China), which was used to evaluate the PM removal performances of the filters developed in this work. The neutralized solid and oil aerosol particles with a mass mean diameter of 300 nm were generated by the aerosol generator using pre-prepared NaCl or Paraffin solutions. The particle counters and pressure transmitters accurately measured the particle concentrations and pressures of the upstream before filter and the downstream after filter at a controllable airflow rate, respectively. The effective area of testing membrane was 100 cm^2. In order to analyze the performances of air filters under different air speeds and compare with the air filters reported in previous literatures, as-developed air filter were tested under the airflow rates of 4.2, 8.5, 12.7 and 17 cm s^{-1} [29,30].

The filtration efficiency (η, %) can be obtained according to the particle concentrations of the upstream and downstream by the following equation [12,16,31,32],

$$\eta = 1 - \frac{C_{downstream}}{C_{upstream}} \quad (2)$$

where $C_{downstream}$ and $C_{upstream}$ are the particle concentrations of the downstream and upstream, respectively.

The pressure drop (ΔP, Pa) of a filter can be obtained from the difference between the upstream and downstream pressures according to the following equation [33],

$$\Delta P = P_{upstream} - P_{downstream} \quad (3)$$

where $P_{downstream}$ (Pa) and $P_{upstream}$ (Pa) are the downstream and upstream pressures, respectively.

The quality factor (QF, Pa^{-1}) can be considered as a benefit-to-cost ratio between filtration efficiency (benefit) and pressure drop (cost). The QF can be obtained based on filtration efficiency (η) and pressure drop (ΔP) as described in Eq. (4) [18,33,34],

$$QF = 1 - \frac{-\ln(1-\eta)}{\Delta P} \quad (4)$$

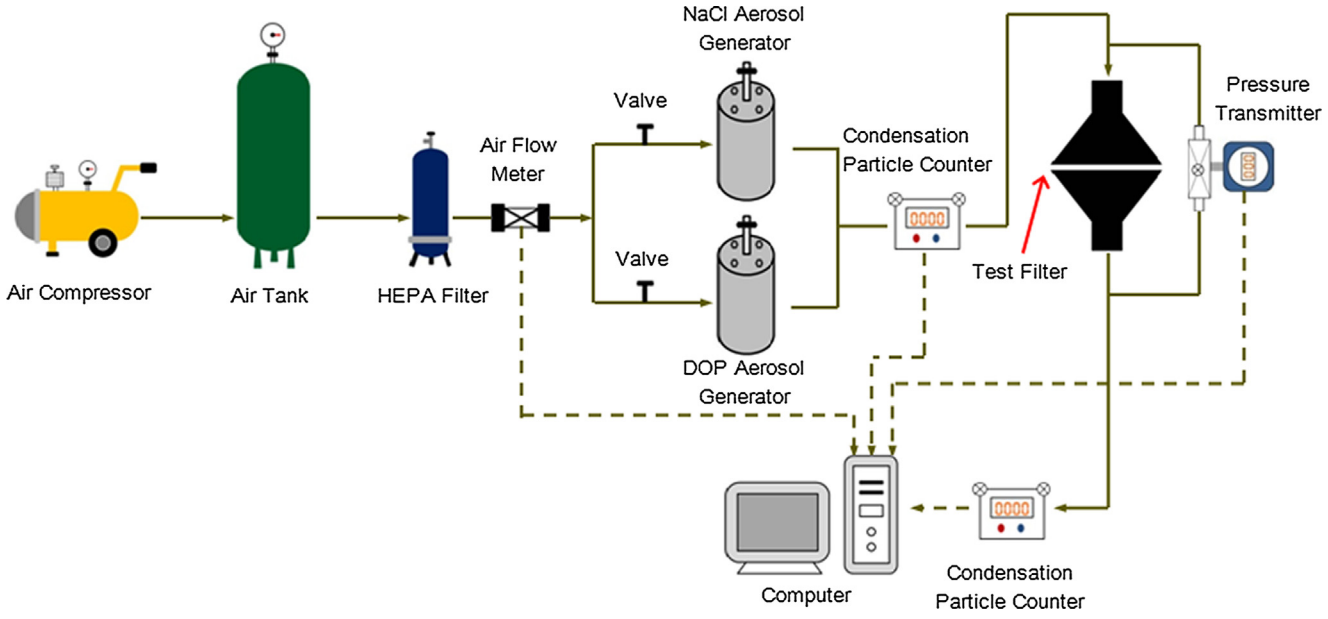

Fig. 1. Scheme of the automatic filtration tester.

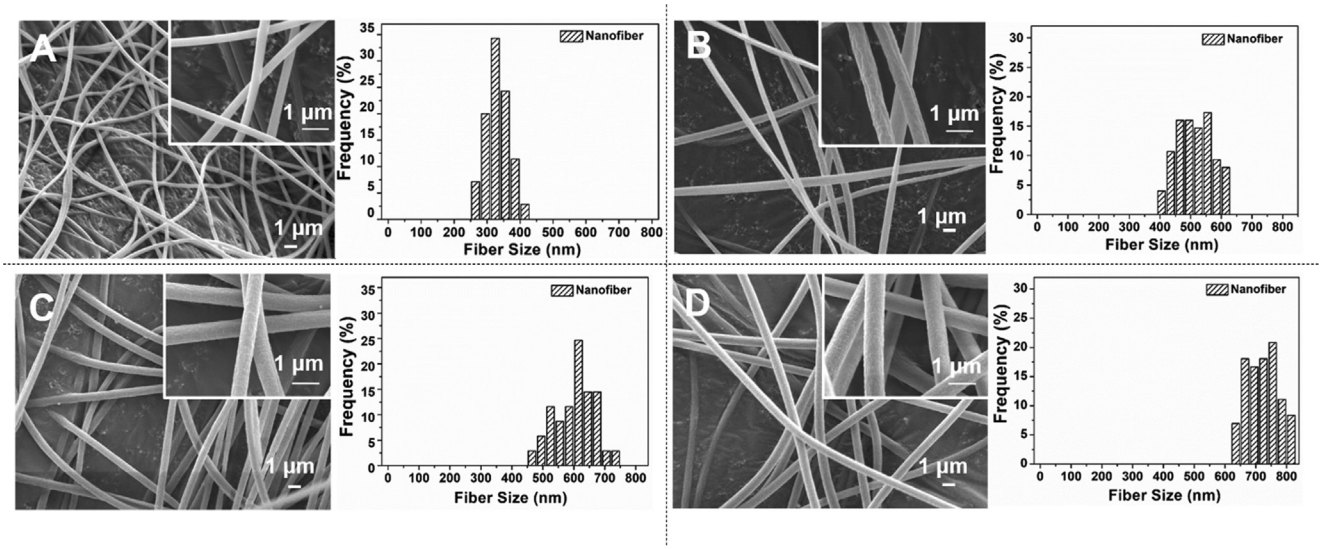

Fig. 2. Surface morphologies of electrospun PAN nanofibrous filters using the 11 wt% PAN solution at different humidity and their respective nanofiber diameter distributions: (A) #P11-3 at RH of 30%; (B) #P11-4 at RH of 40%; (C) #P11-5 at RH of 50%; (D) #P11-6 at RH of 60%.

3. Results and discussion

3.1. Development of bead-free and bead-on-string nanofibrous filters

3.1.1. Morphologies of the nanofibrous filters

The surface morphologies of the air filters prepared by electrospinning PAN solutions with different concentrations at various humidity were observed by FESEM as shown in Figs. 2–4. As shown in Fig. 2, the filters developed by electrospinning the 11 wt% PAN solution are all composed of uniform bead-free nanofibers, which should be attributed to the sufficient concentration/viscosity of dope solution. The average nanofiber diameters of #P11-3 fabricated at RH of 30%, #P11-4 at RH of 40%, #P11-5 at RH of 50% and #P11-6 at RH of 60%, are 340 ± 3 nm, 523 ± 23 nm, 614 ± 10 nm and 750 ± 12 nm as summarized in Table 2. With the elevation of RH, the average diameters of nanofibers are increased.

In order to acquire thinner nanofibers, the PAN concentration of electrospun dope solution was reduced to 8 wt%. As shown in Fig. 3A, the filter #P8-3 electrospun using the 8 wt% PAN dope at RH of 30% exhibits a bead-on-string structure while the other filters developed at RH of 40% (#P8-4), 50% (#P8-5) and 60% (#P8-6) display uniform nanofibrous structures as shown in Fig. 3B–D. The mechanism of the bead-on-string structure generation will be discussed in the next section. The average nanofiber diameter of #P8-3 is 82 ± 5 nm while the average nanobead diameter is 337 ± 13 nm (Table 2). Besides, the average nanofiber diameters of #P8-4, #P8-5 and #P8-6 are 232 ± 16, 289 ± 25 and 371 ± 9 nm, respectively.

Although the ultrafine PAN nanofibrous filters obtained by electrospinning the 8 wt% solution may possess superior capture efficiency of ultrafine PM, they tend to show high airflow resistance due to the high nanofiber packing density. Thus, hierarchically bead-on-string filters are proposed and developed in this work to achieve an excellent ultrafine PM removal efficiency as well as a low airflow resistance. Fig. 4 shows the surface morphologies of the filters fabricated by electrospinning the 8 wt% and 5 wt% PAN dopes simultaneously and their diameter distributions of nanofibers and nanobeads. The nanofibers fabricated by electrospinning the 8 wt% PAN are supposed to afford sufficient mechanical properties while the bead-on-string

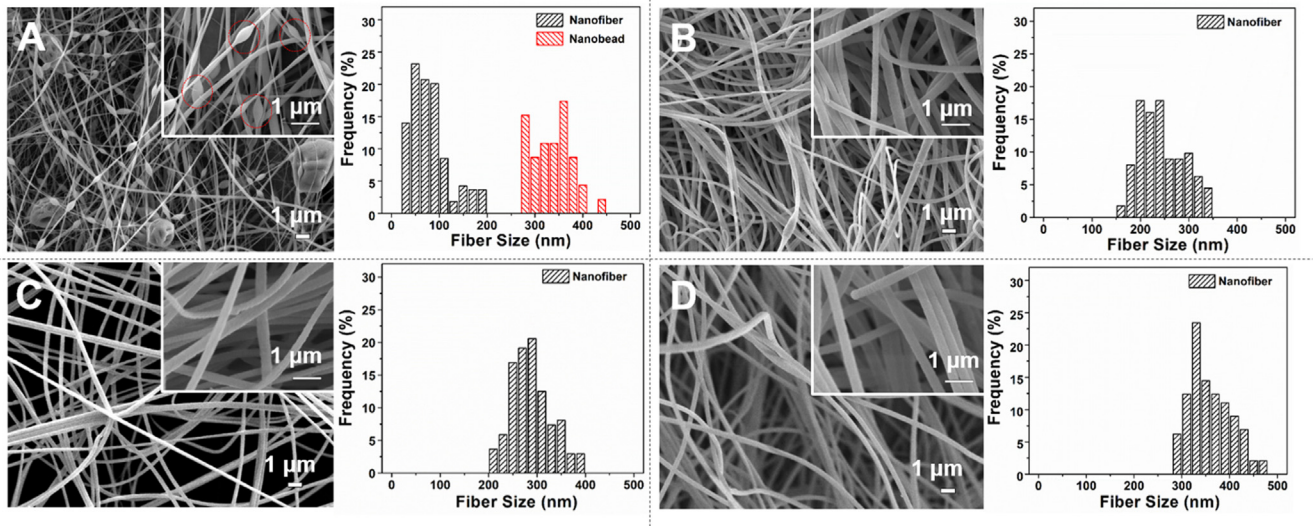

Fig. 3. Surface morphologies of electrospun PAN filters developed by electrospinning the 8 wt% PAN solution at different humidity and their respective diameter distributions: (A) #P8-3 at RH of 30%; (B) #P8-4 at RH of 40%; (C) #P8-5 at RH of 50%; (D) #P8-6 at RH of 60%.

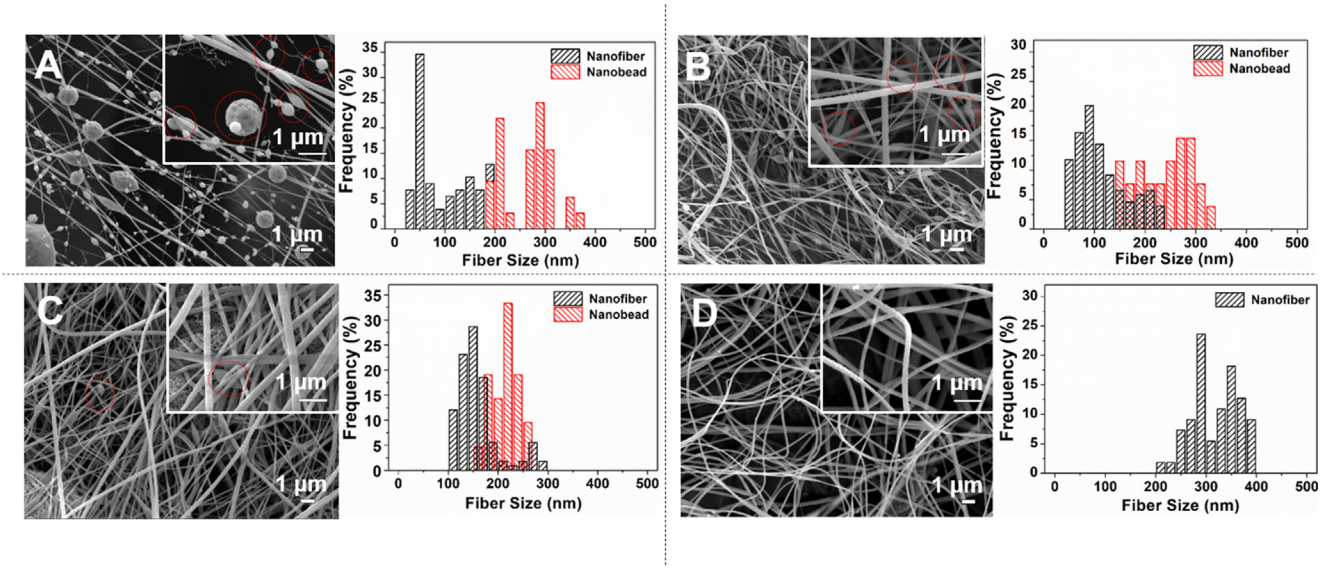

Fig. 4. Surface morphologies of electrospun PAN filters using 8 wt% and 5 wt% PAN solutions at different humidity and their respective diameter distributions: (A) #P8/5-3 at RH of 30%; (B) #P8/5-4 at RH of 40%; (C) #P8/5-5 at RH of 50%; (D) #P8/5-6 at RH of 60%.

nanofibers developed by electrospinning the 5 wt% PAN are designed to guarantee the PM removal efficiencies. As shown in Fig. 4A-C, the filters #P8/5-3, #P8/5-4 and #P8/5-5 show remarkable bead-on-string morphologies. Along with the increase in RH, the nanobead densities of the filter are decreased from 4.5×10^5 (RH = 30%) to 1.6×10^5 (RH = 40%), and further down to 0.42×10^5 as the RH was increased to 50% (Fig. 5). Besides, according to the images shown in Fig. 4D, the filter #P8/5-6 exhibits a uniform bead-free nanofibrous structure with a nanofiber diameter of 283 ± 9 nm.

3.1.2. Generation mechanisms of the bead-on-string structure

During the electrospinning process, the nanofibers and nanobeads are generated after onset of ejection and rectilinear jet development, elongation and bending deformation of jet, and nanofiber solidification with solvent evaporation under an electrical field [35]. The crucial parameters including intrinsic properties of polymeric dopes, operational parameters and surrounding ambient conditions have been optimized to investigate their effects on resultant nanofibers [36]. The morphologies of nanofibers are primarily decided by the dope compositions [37]. For a given pair of polymer and solvent, a minimum polymer concentration is required to fabricate successful nanofibers [38–40]. In this work, all the dope solutions exhibit sufficient concentrations to form bead-free nanofibers. Under the RH of 30%, the filter structure tended to transform from spherical bead-on-string structure (Fig. 4A) to spindle-like bead-on-string morphology (Fig. 3A) and eventually bead-free uniform nanofibers (Fig. 2A) with the elevation of PAN concentrations. At other RH conditions, the average diameter of nanofibers is enhanced with increasing of polymer concentration. The mechanism is that the increase of polymer concentration is able to strengthen the polymer chain entanglement in the jets which are ejected from the Taylor cone on the spinnerets under an electrical field [41]. When the retractive force of jets due to macromolecular entanglement achieves a good balance with the Coulombic stretching force, the stable jets can produce continuous nanofibers [40]. In contrast, if there is not sufficient intermolecular force to stabilize the jets due to a low polymer concentration, the destabilized jets are prone to generate a bead-on-string structure and even break-up into spherical fiber-free beads [40].

Compared to the intrinsic properties of dope solutions, much less efforts have been devoted in investigating the effects of surrounding ambient conditions such as humidity on the electrospun filters [35,40,42]. However, the results in this work demonstrate that the optimization of humidity condition is crucial to control the morphologies of the filters. The charges carried on the nanofibers tend to be discharged at a higher RH as they can be captured by the water vapor in the surrounding ambient, which lead to a weaker repulsive force on the jets and thicker nanofibers in consequence [43,44]. In contrast, more charges are able to stay on the nanofibers at a lower RH, which force the jets undergo a stronger drawdown force and thus thinner nanofibers. As the polymer concentration is decreased (5 wt% in this work), the unbalanced status between repulsive and constrictive forces produce bead-on-string morphologies as shown in Fig. 4A-C. Meanwhile, more water vapor in the ambient condition at a higher RH could promote the precipitation of PAN due to a nonsolvent-induced phase inversion phenomenon, which prohibits the elongation of jets and locks in the nanofiber diameter [42,44,45]. Thus, nanofibers with larger diameters tend to be produced at a higher RH.

3.2. Filtration efficiency and air drop of as-developed filters

The removal of aerosol PMs by fibrous membranes comply with several mechanisms including gravity settling, electrostatic attraction, inertial impaction, physical interception and Brownian diffusion [46]. The diffusion and interception mechanisms play primary functions in intercepting ultrafine PMs with a diameter below 300 nm while the particles with a diameter between 300 and 1000 nm respond to gravity setting and inertial impaction mechanisms [47]. Among all aerosol PMs, ultrafine particles with diameter of 300 nm have the lowest removal efficiency. Thus, the PM removal efficiency of fibrous filters could form a distinctive lognormal curve, the lowest point at 300 nm of which is the minimal capture efficiency of the most penetrating particle size (MPPS) [48]. Therefore, all filters prepared in this work were evaluated by NaCl solid and Paraffin oil aerosols with an average diameter of 300 nm [49].

3.2.1. Bead-free nanofibrous filters

As shown in Fig. 6, when the airflow rate was 4.2 cm s^{-1}, the filters fabricated by the 11 wt% PAN solution exhibited removal efficiencies of 84.7 ± 1.2% (#P11-3), 71.3 ± 1.1% (#P11-4), 53.3 ± 3.6% (#P11-5) and 51.7 ± 2.9% (#P11-6) towards 300 nm NaCl aerosols while their corresponding pressure drops were 10.3 ± 0.6, 4.7 ± 0.5, 2.7 ± 0.6 and 3.3 ± 0.6 Pa. As the nanofiber diameters were further reduced to 289 ± 25 nm (#P8-5) and 232 ± 16 nm (#P8-4), the air filters were able to achieve higher solid aerosol removal efficiencies of

Table 2
Properties of the PAN air filters developed in this work.

Membrane Name	Intrinsic Membrane Properties			Air Filter Test Properties							Mechanical Properties		
	Average Nanofiber Diameter (nm)	Average Nanobead Diameter (nm)	Weight Basis ($g\ m^{-2}$)	E (%) NaCl	ΔP (Pa) NaCl	E (%) Paraffin	ΔP (Pa) Paraffin	V ($cm\ s^{-1}$)	Q_f (Pa^{-1}) NaCl	Q_f (Pa^{-1}) Paraffin	Tensile Module (MPa)	Tensile at Break (MPa)	Elongation at Break (%)
#P11-3	340 ± 3	–	1.77	84.7 ± 1.2	10.3 ± 0.6	75.3 ± 1.1	10.0 ± 0.1	4.2	0.24 ± 0.01	0.18 ± 0.02	0.20 ± 0.01	3.2 ± 0.2	47.9 ± 1.2
#P11-4	523 ± 23	–		71.3 ± 1.1	4.7 ± 0.5	50.0 ± 1.1	3.0 ± 0.1		0.19 ± 0.01	0.17 ± 0.02	0.21 ± 0.06	4.1 ± 0.2	56.7 ± 1.7
#P11-5	614 ± 10	–		53.3 ± 3.6	2.7 ± 0.6	33.0 ± 8.8	3.0 ± 0.1		0.16 ± 0.01	0.16 ± 0.01	0.24 ± 0.04	3.5 ± 0.1	51.6 ± 0.8
#P11-6	750 ± 12	–		51.7 ± 2.9	3.3 ± 0.6	25.4 ± 6.7	3.0 ± 0.1		0.15 ± 0.01	0.12 ± 0.01	0.22 ± 0.05	4.1 ± 0.7	65.9 ± 0.6
#P8-3	82 ± 5	337 ± 13	1.77	95.0 ± 0.1	17.3 ± 0.6	90.6 ± 1.3	17.3 ± 0.6	4.2	0.17 ± 0.01	0.14 ± 0.01	0.23 ± 0.02	2.6 ± 0.3	49.2 ± 2.1
#P8-4	232 ± 16	–		93.6 ± 1.2	18.0 ± 0.1	89.8 ± 1.1	17.0 ± 0.1		0.15 ± 0.01	0.14 ± 0.01	0.23 ± 0.04	3.5 ± 0.1	46.4 ± 2.8
#P8-5	289 ± 25	–		86.3 ± 1.2	13.0 ± 0.1	82.7 ± 0.5	12.7 ± 0.6		0.15 ± 0.01	0.14 ± 0.01	0.21 ± 0.02	2.8 ± 0.1	64.0 ± 1.1
#P8-6	371 ± 9	–		81.7 ± 1.5	10.0 ± 0.1	74.3 ± 4.3	8.3 ± 0.6		0.17 ± 0.01	0.16 ± 0.01	0.19 ± 0.01	2.9 ± 0.1	53.0 ± 3.7
#P8/5-3	70 ± 9	249 ± 7	1.77	96.5 ± 0.9	14.3 ± 0.6	91.9 ± 2.3	14.0 ± 0.1	4.2	0.19 ± 0.01	0.14 ± 0.01	0.15 ± 0.03	2.7 ± 0.1	57.6 ± 3.3
#P8/5-4	118 ± 10	220 ± 4		95.6 ± 1.0	16.3 ± 0.6	91.3 ± 1.7	14.6 ± 0.6		0.31 ± 0.01	0.23 ± 0.01	0.19 ± 0.02	3.2 ± 0.1	57.2 ± 0.4
#P8/5-5	152 ± 4	236 ± 9		92.7 ± 0.6	16.0 ± 0.1	87.3 ± 1.0	13.3 ± 0.6		0.23 ± 0.11	0.14 ± 0.06	0.20 ± 0.01	3.6 ± 0.3	50.5 ± 1.4
#P8/5-6	283 ± 9	–		90.0 ± 0.1	15.6 ± 0.6	83.7 ± 3.2	15.3 ± 0.6		0.24 ± 0.02	0.10 ± 0.03	0.22 ± 0.05	4.4 ± 0.2	64.2 ± 0.9

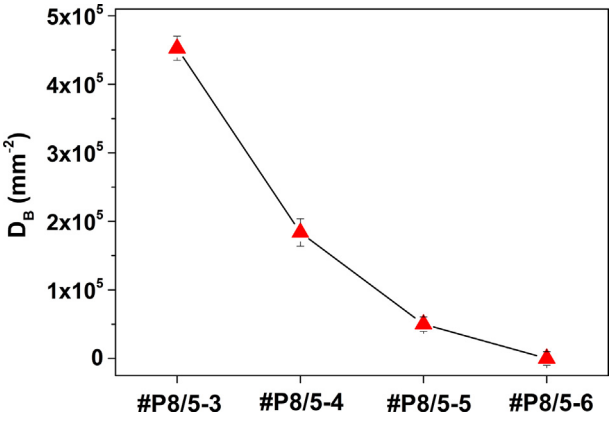

Fig. 5. The nanobead densities of the PAN air filters fabricated by electrospinning the 8 wt% and 5 wt% PAN solutions.

86.3 ± 1.2% and 93.6 ± 1.2% while the air pressure drops were 13.0 ± 0.1 and 18.0 ± 0.1 Pa, respectively (Fig. 7). It indicates that the air filter with a thinner nanofiber diameter exhibits higher removal efficiency as well as higher airflow resistance.

The same trend could be observed when the filters were utilized to capture Paraffin oil aerosols. As shown in Fig. 6, the oil aerosol removal efficiencies of the filters developed from 11 wt% PAN solution could be enhanced from 25.4 ± 6.7% (#P11-6 with an average diameter of 750 ± 12 nm) to 75.3 ± 1.1% (#P11-3 with an average diameter of 340 ± 3 nm) while the pressure drops were increased from 3.0 ± 0.1 to 10.0 ± 0.1 Pa. The filters developed using the 8 wt% PAN dope could obtain higher oil aerosol removal efficiencies of 89.8 ± 1.1% (#P8-4 with an average diameter of 232 ± 16 nm) and 82.7 ± 0.5% (#P8-5 with an average diameter of 289 ± 25 nm) due to their thinner nanofibers (Fig. 7). Noted that the removal efficiencies of all filters for oil aerosols were lower than those for solid aerosols, especially for the filters composed of nanofibers with larger diameters. This phenomenon should be due to the fact that the oil particles require more contact time to be captured by nanofibers, which thus result in a lower efficiency at the same airflow rate [50].

The filtration efficiency (η) of a fibrous filter can be anticipated by following equation [51]:

$$\eta = 1 - \exp[-\frac{4\alpha\eta_f Z}{\pi(1-\alpha)d_f}] \quad (5)$$

where α is the fiber packing density, η_f is the single fiber efficiency, Z is the filter thickness and d_f is the mean fiber diameter. According to the above equation, the filtration efficiency of filters exhibits a positive correlation with fiber packing density and single fiber efficiency, a negative correlation with filter thickness and mean fiber diameter. In addition, the nanofibers with smaller diameters enhance the single fiber efficiency η_f by improving both diffusion and interception capture abilities [8]. Thus, for the filters with the same thickness and packing density, the reduction of nanofiber diameter could enhance the filtration efficiency significantly. Moreover, with the increasing of airflow rate, the filtration efficiencies were reduced for both solid and oil aerosols as shown in Figs. 6 and 7. A higher airflow rate prohibits the sufficient retention time of aerosols in the nanofibrous filter, which reduces the opportunities of aerosols to interact with nanofibers *via* Brownian diffusion [8]. Thus, all the removal efficiencies decreased with increasing of airflow rates.

Nonetheless, the thinner nanofibers not only lead to a higher PM removal efficiency but also give rise to a higher airflow resistance rendering a larger pressure drop. At the same airflow rate of 4.2 cm s^{-1}, with the reduction of nanofiber diameter from 750 ± 12 nm (#P11-6) to 232 ± 12 nm (#P8-4), the pressure drop increased from 3.3 ± 0.6 Pa (#P11-6) to 18.0 ± 0.1 Pa (#P8-4) when filtrating solid

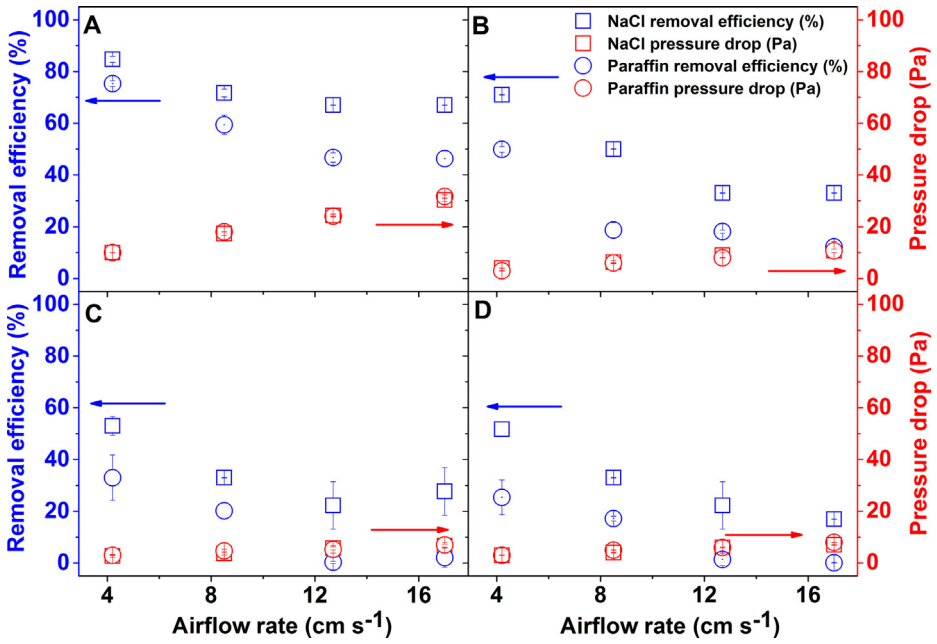

Fig. 6. The removal efficiencies and pressure drops of the air filters developed by electrospinning the 11 wt% PAN solution when the upstream air contained NaCl solid or Paraffin oil aerosols with an average diameter of 300 nm at different airflow rates: (A) #P11-3; (B) #P11-4; (C) #P11-5; (D) #P11-6.

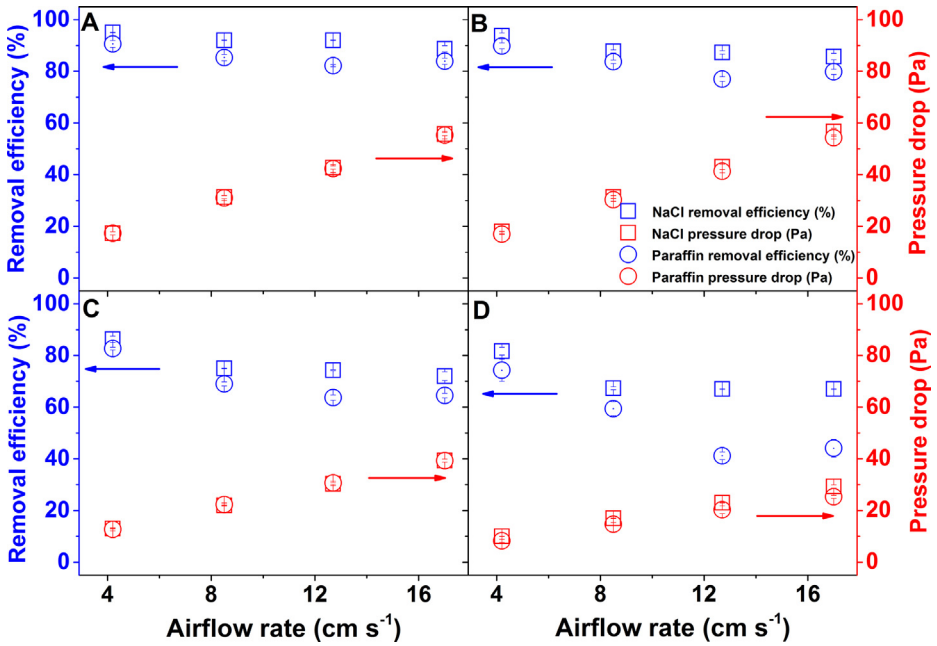

Fig. 7. The removal efficiencies and pressure drops of the air filters developed by electrospinning the 8 wt% PAN solution when the upstream air contained NaCl solid or Paraffin oil aerosols with an average diameter of 300 nm at different airflow rates: (A) #P8-3; (B) #P8-4; (C) #P8-5; (D) #P8-6.

aerosols. The pressure drop raised from 3.0 ± 0.1 Pa (#P11-6) to 17.0 ± 0.1 Pa (#P8-4) when removing oil aerosols. Moreover, the pressure drops of all filters exhibit a nearly linear positive correlation with the airflow rate, which is consistent with Darcy's law for viscous resistance [8]. The pressure drop ΔP across a nanofibrous filter can be estimated by a revised Davies' empirical formula as following [52,53]:

$$\Delta P = \frac{64\mu U_0 W\alpha^{0.5}(1 + 56\alpha^3)}{d_f^2 \rho_f}$$

where μ is the air dynamic viscosity, U_0 is the airflow rate, W is the basis weight of filter, ρ_f is the filter material density. According to the above equation, the pressure drop ΔP shows a proportional relation with the airflow rate and an inverse relation with the square of nanofiber diameter, which is in good consistence with the experimental results.

3.2.2. *Bead-on-string nanofibrous filters*

In order to achieve air filters possessing both higher removal efficiencies and low pressure drops, the bead-on-string filters #P8/5-3, #P8/5-4 and #P8/5-5 were developed in this work. The filtration efficiencies and pressure drop properties of these filters were examined as shown in Fig. 8. The bead-on-string filters exhibit the same trends as nanofibrous filters: with the increasing of airflow rates, the PM removal efficiencies were reduced while the pressure drops were increased. In contrast to nanofibrous filters (such as #P8-4 with solid and oil aerosols

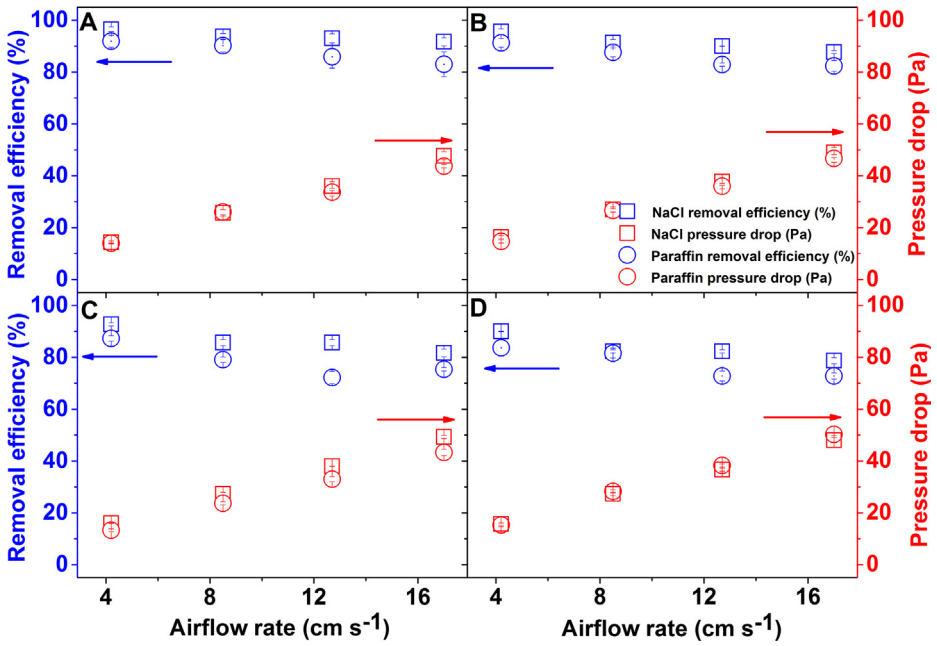

Fig. 8. The removal efficiencies and pressure drops of the air filters developed by electrospinning 5 wt% and 8 wt% PAN solutions simultaneously at different airflow rates: (A) #P8/5-3; (B) #P8/5-4; (C) #P8/5-5; (D) #P8/5-6.

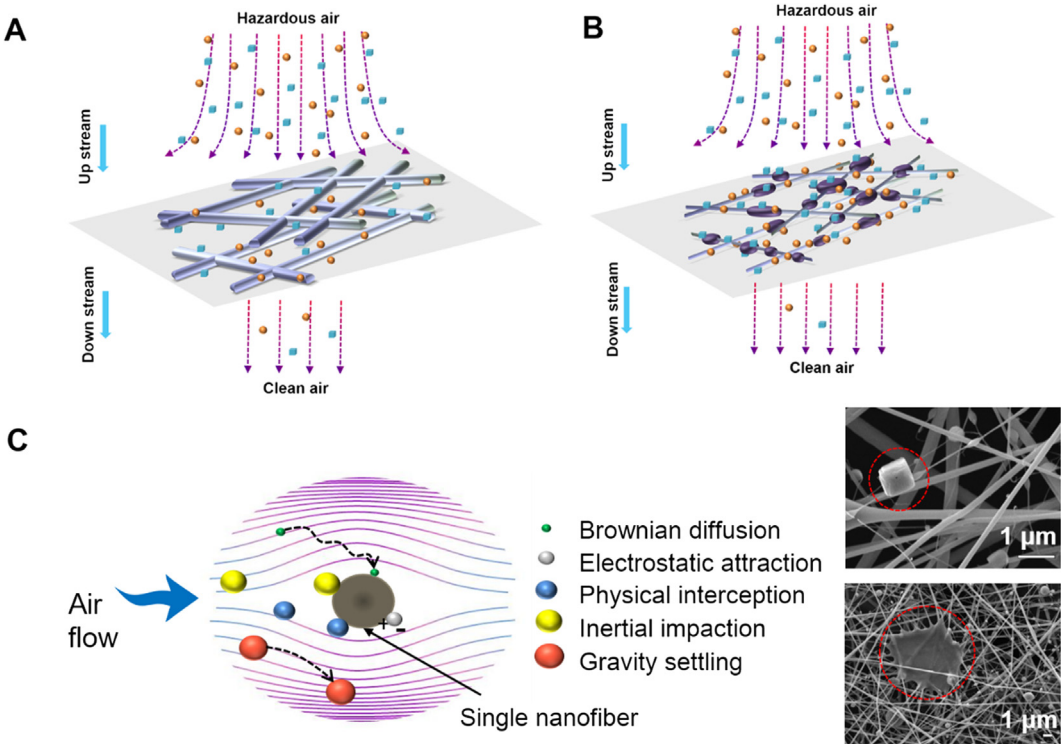

Fig. 9. The schematic diagrams of air filtration through (A) nanofibrous and (B) bead-on-string filters; (C) the interception mechanisms of in-air PMs *via* a single nanofiber, the inserted FESEM images show the surface morphologies of nanofibers after capturing NaCl solid PM (top) and Paraffin oil PM (bottom).

removal efficiencies of 93.6 ± 1.2% and 89.8 ± 1.1%), the bead-on-string filters #P8/5-3 (Fig. 8A) possess higher removal efficiencies of 96.5 ± 0.9% and 91.9 ± 2.3% towards solid and oil aerosols, respectively. Meanwhile, compared to the nanofibrous filters (such as #P8-4 with pressure drops of 18.0 ± 0.1 and 17.0 ± 0.1 Pa towards solid and oil aerosols), it shows lower pressure drops of 14.3 ± 0.6 and 14.0 ± 0.1 Pa towards solid and oil aerosols, respectively. In addition, as the nanofiber diameters of #P8/5-4 and #P8/5-5 increased to 118 ± 10 and 152 ± 4 nm, nanobead diameters reduced to 220 ± 4 and 236 ± 9 nm, the solid and oil aerosols removal efficiencies at the airflow rate of 4.2 cm s^{-1} were reduced while the pressure drops were increased as shown in Fig. 8B-C and summarized in Table 2. When the filter was transformed from a bead-on-string structure to a bead-free nanofibrous morphology (#P8/5-6), the solid and oil aerosols removal efficiencies were further decreased to 90.0 ± 0.1% and 83.7 ± 3.2% as shown in Fig. 8D, demonstrating the importance of the bead-on-string structure in fabrication of highly efficient filters for air filtration applications.

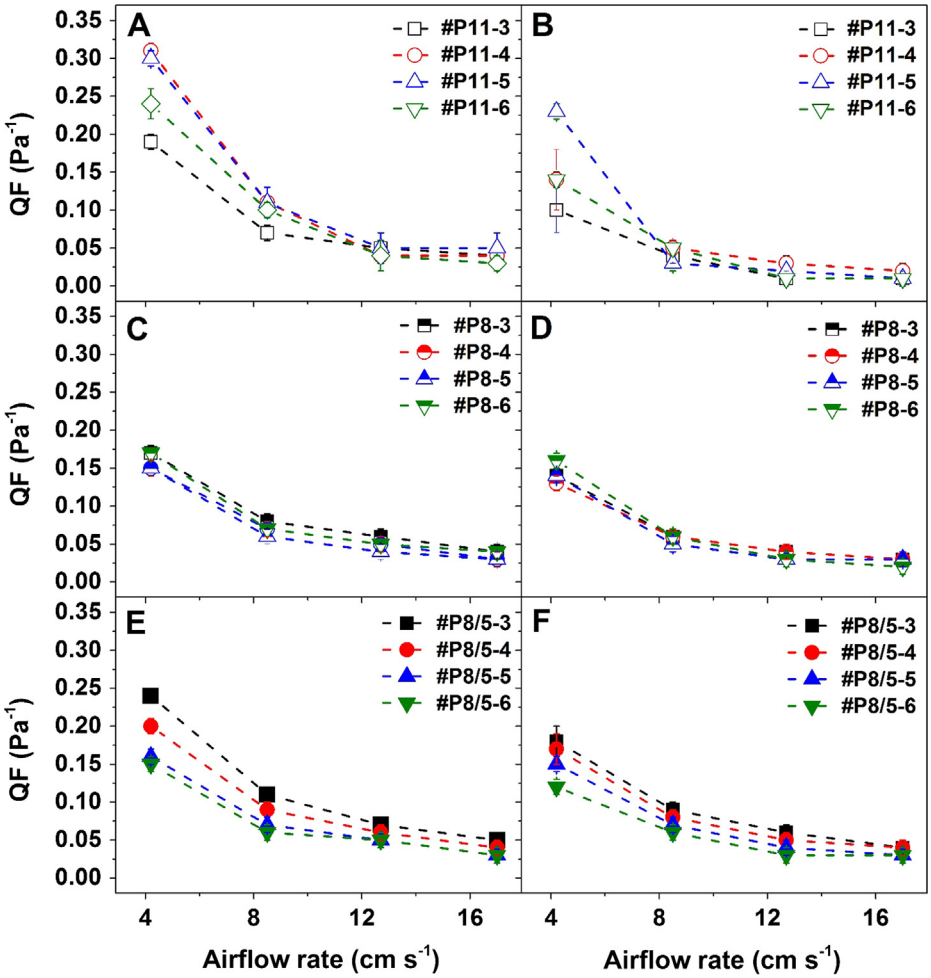

Fig. 10. QFs of PAN filters developed by electrospinning different PAN solutions at various airflow rates: filters developed by electrospinning the 11 wt% PAN solution (A: treating NaCl solid aerosols, B: treating Paraffin oil aerosols), 8 wt% PAN solution (C: treating NaCl solid aerosols, D: treating Paraffin oil aerosols), 5 wt % and 8 wt% PAN solutions (E: treating NaCl solid aerosols, F: treating Paraffin oil aerosols).

3.2.3. Mechanisms of the effective PM capture by bead-on-string nanofibrous filters

Compared to the filters with compacted nanofibrous structures shown in Fig. 9A, the excellent removal efficiencies and ultralow pressure drops of the bead-on-string filters should be contributed to the mechanism that ultrathin nanofibers are capable to intercept PM effectively while the nano-sized beads reduce packing density and alleviate the filter resistance (Fig. 9B). As shown in Fig. 9C, the ultrafine nanofibers effectively remove the PM in air following the mechanisms of Brown diffusion, electrostatic attraction, physical interception, inertial impaction and gravity settling. The solid aerosol particles were effectively captured on the single nanofiber surface as shown in the inserted images in Fig. 9C (top). In contrast, as oil PM can coalesce and flow, their loading behaviors include deposition on nanofiber, surrounding nanofiber and accumulation on nanofibrous surface. As shown in the inserted image at the bottom of Fig. 9C, a liquid film at nanofiber intersections appear with the accumulation of oil aerosols.

3.3. Quality factors (QF) of as-developed filters

To evaluate the benefit-to-cost ratios of all filters, the QF values are calculated and shown in Fig. 10. Albeit that the nanofibrous filters fabricated by electrospinning 11 wt% PAN solution exhibit low removal efficiencies, they possess high QF values due to their low pressure drops as shown in Fig. 10A-B. All the filters developed at lower RH possess higher QFs (Fig. 10A-F). It should be attributed to their higher removal efficiencies even though they showed higher pressure drops. Although the bead-on-string filters show lower QF values (Fig. 10E-F) that the QF values of nanofibrous filters, they still possess competitive QF values between 0.15 and 0.25 Pa^{-1} when filtrating 300 nm NaCl solid aerosols and from 0.13 to 0.20 Pa^{-1} when filtrating 300 nm Paraffin oil aerosols at an airflow rate of 4.2 cm s^{-1}. In particular, the QF values of #P8/5-3 towards solid and oil aerosols are 0.19 ± 0.01 and 0.14 ± 0.01 Pa^{-1} at an airflow rate of 4.2 cm s^{-1}, which is higher that the QF values of the filters reported in most literatures (usually < 0.15 Pa^{-1}) [33,34,54–56].

3.4. Robustness of the air filter

On the basis of the excellent filtration performance of the bead-on-string filter #P8/5-3, a bead-on-string filter with a higher mass weight of 3.10 g m^{-2} was developed by extending electrospinning time for practical examinations. As shown in Fig. 11A, the filter can easily achieve a removal filtration above 99% by increasing the mass weight of the filter. It shows a stable removal efficiency of 99.3 ± 0.2% and a pressure drop of 27.0 ± 0.1 Pa for 30 testing cycles, which attests the robustness of the filter in long-term usage. To compare with commercial filters and air filters reported in literatures, the filtration efficiencies versus their pressure drops at an airflow rate around 4.2 cm s^{-1} are plotted in Fig. 11B [15,27,54,57–63]. The bead-on-string filter developed in this work shows a highly competitive performance with an outstanding removal efficiency and a low pressure drop. Moreover, in

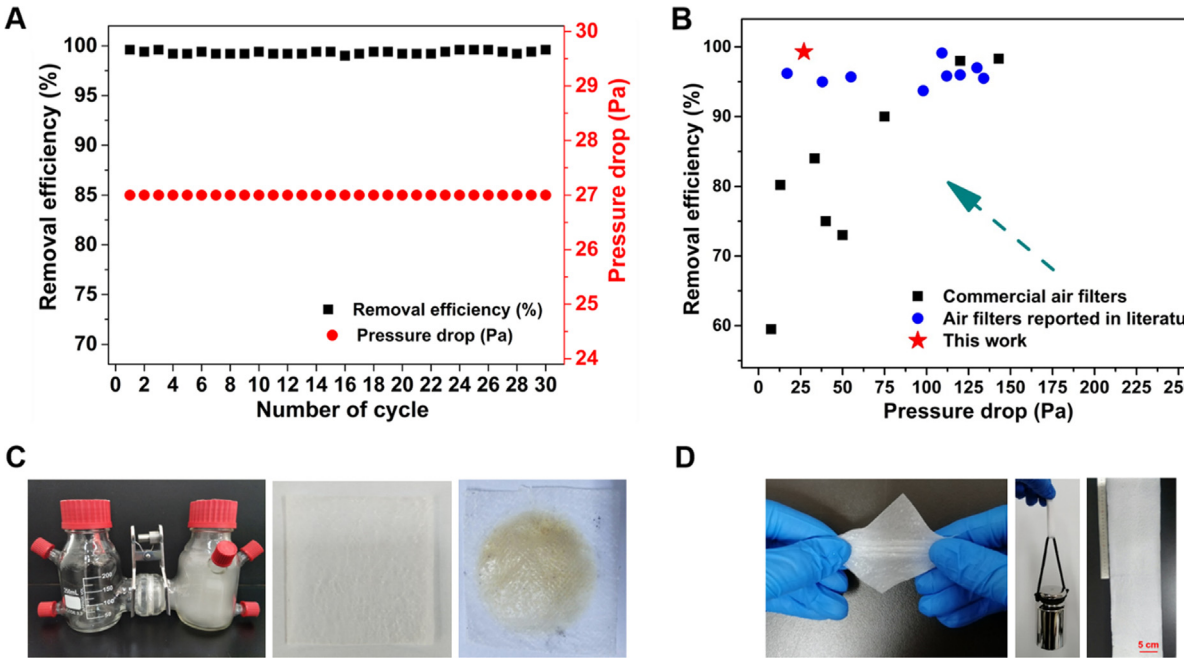

Fig. 11. (A) Filtration efficiencies of an bead-on-string filter in 30 cycles; (B) Comparison figure of the bead-on-string filter with other filters reported in literatures and commercial filters; (C) Demonstration of the filter to shut off smoke PM from outdoor (right bottle) from entering the indoor environment (left bottle); (D) images of a twisted, stretching and large-scale filter developed in this work.

order to testify the filter in practical applications, it was fixed between smoke generated by cigarette (right bottle) and clean air (left bottle) as shown in Fig. 11C. It provides an obvious demonstration that the filter has blocked the PM particles in the right bottle from entering the indoor clean environment in the left bottle. After 24 h, the left bottle is still transparent, indicating the as-prepared filter is capable to provide long-term protection and be used as window screens. The images shown in Fig. 11C illustrate that the filter turned brown after 24 h as it has effectively captured the PM particles. Meanwhile, the filters developed in this work can endure twisting without obvious weight loss and withstand the stretching by autoclave (Fig. 11D). As summarized in Table 2, all filters exhibited tensile modules about 0.2 Mpa and tensile strengths around 3.0 Mpa, which are sufficient for air filtration applications. Meanwhile, these filters are facile to be scaled up for large-scale applications.

4. Conclusions

In summary, the bead-on-string PAN filters developed by electrospinning are demonstrated to be excellent air filters to capture the ultrafine solid and oil PM in the air. Attributed to the optimizations of concentration/viscosity of PAN dope and RH conditions, the imbalance between the repulsive force from applied electric field and restrictive force from jet surface tension generate the desirable bead-on-string morphologies. The outstanding removal efficiencies should be benefited from the ultrafine nanofibers between the beads while the low airflow resistance should be due to the open interconnected airflow channels constructed by the nanobeads. By optimizing the mass weight, the bead-on-sting filter could easily attain an outstanding removal efficiency over 99% and a low pressure drop of 27 Pa, which is more competitive than commercial filters and filters reported in the literatures. Besides, the resultant filter achieved excellent performance, reusability and sufficient mechanical robustness for practical applications. Moreover, the filters can be easy to be scaled up without utilization of special post-treatment/modifications and costly materials. In consequence, the filters designed and developed in this work can be promising candidates in various air filtration applications including respiration, window screen, and medical equipment.

CRediT authorship contribution statement

Jinhui Jeanne Huang: Resources, Project administration, Funding acquisition. **Yuxiao Tian:** Validation, Investigation, Data curation. **Rong Wang:** Writing - review & editing. **Miao Tian:** Data curation, Resources. **Yuan Liao:** Conceptualization, Methodology, Writing - original draft, Visualization, Supervision.

Declaration of Competing Interest

The authors declare that they have no known competing financial interests or personal relationships that could have appeared to influence the work reported in this paper.

Acknowledgment

This work was supported by the National Key Research and Development Program of China (2016YFC0400709), National Science Foundation of Tianjin (18JCYBJC41900), National Natural Science Foundation of China (21906086), the Fundamental Research Funds for the Central Universities, Nankai University (040-63191433).

References

[1] Q. Zhang, X. Jiang, D. Tong, S.J. Davis, H. Zhao, G. Geng, T. Feng, B. Zheng, Z. Lu, D.G. Streets, R. Ni, M. Brauer, A. van Donkelaar, R.V. Martin, H. Huo, Z. Liu, D. Pan, H. Kan, Y. Yan, J. Lin, K. He, D. Guan, Transboundary health impacts of transported global air pollution and international trade, Nature 543 (2017) 705.
[2] T. Xue, T. Zhu, Y. Zheng, Q. Zhang, Declines in mental health associated with air pollution and temperature variability in China, Nat. Commun. 10 (2019) 2165.
[3] P. Fu, X. Jiang, L. Ma, Q. Yang, Z. Bai, X. Yang, J. Chen, W. Yuan, H. Wang, W. Lv, Enhancement of PM2.5 Cyclone Separation by Droplet Capture and Particle Sorting, Environ. Sci. Technol. 52 (2018) 11652–11659.
[4] S. Schiller, H.-J. Schmid, Highly efficient filtration of ultrafine dust in baghouse filters using precoat materials, Powder Technol. 279 (2015) 96–105.
[5] P. Fu, F. Wang, L. Ma, X. Yang, H. Wang, Fine particle sorting and classification in the cyclonic centrifugal field, Sep. Purif. Technol. 158 (2016) 357–366.
[6] P. Saiyasitpanich, T. Keener, M. Lu, S.-J. Khang, D. Evans, Collection of ultrafine Diesel Particulate Matter (DPM) in cylindrical single-stage wet electrostatic, Precipitators (2007).
[7] R. Al-Attabi, Y. Morsi, W. Kujawski, L. Kong, J.A. Schütz, L.F. Dumée, Wrinkled silica doped electrospun nano-fiber membranes with engineered roughness for

advanced aerosol air filtration, Sep. Purif. Technol. 215 (2019) 500–507.
[8] C.-H. Hung, W.W.-F. Leung, Filtration of nano-aerosol using nanofiber filter under low Peclet number and transitional flow regime, Sep. Purif. Technol. 79 (2011) 34–42.
[9] J. Liu, F.O. Dunne, X. Fan, X. Fu, W.-H. Zhong, A protein-functionalized microfiber/protein nanofiber Bi-layered air filter with synergistically enhanced filtration performance by a viable method, Sep. Purif. Technol. 229 (2019) 115837.
[10] S. Zhang, N. Tang, L. Cao, X. Yin, J. Yu, B. Ding, Highly integrated polysulfone/polyacrylonitrile/polyamide-6 air filter for multilevel physical sieving airborne particles, ACS Appl Mater Interfaces 8 (2016) 29062–29072.
[11] S. Zhang, H. Liu, X. Yin, J. Yu, B. Ding, Anti-deformed polyacrylonitrile/polysulfone composite membrane with binary structures for effective air filtration, ACS Appl Mater Interfaces 8 (2016) 8086–8095.
[12] A.L. Macfarlane, J.F. Kadla, R.J. Kerekes, High performance air filters produced from freeze-dried fibrillated wood pulp: fiber network compression due to the freezing process, Ind. Eng. Chem. Res. 51 (2012) 10702–10711.
[13] B. Khalid, X. Bai, H. Wei, Y. Huang, H. Wu, Y. Cui, Direct blow-spinning of nanofibers on a window screen for highly efficient PM2.5 removal, Nano Lett. 17 (2017) 1140–1148.
[14] B. Shi, L. Ekberg, Ionizer assisted air filtration for collection of submicron and ultrafine particles-evaluation of long-term performance and influencing factors, Environ. Sci. Technol. 49 (2015) 6891–6898.
[15] J. Kim, S. Chan Hong, G.N. Bae, J.H. Jung, Electrospun magnetic nanoparticle-decorated nanofiber filter and its applications to high-efficiency air filtration, Environ. Sci. Technol. 51 (2017) 11967–11975.
[16] H. Souzandeh, L. Scudiero, Y. Wang, W.-H. Zhong, A disposable multi-functional air filter: paper towel/protein nanofibers with gradient porous structures for capturing pollutants of broad species and sizes, ACS Sustain. Chem. Eng. 5 (2017) 6209–6217.
[17] C. Liu, P.-C. Hsu, H.-W. Lee, M. Ye, G. Zheng, N. Liu, W. Li, Y. Cui, Transparent air filter for high-efficiency PM2.5 capture, Nat. Commun. 6 (2015) 6205.
[18] Q. Zhang, Q. Li, T.M. Young, D.P. Harper, S. Wang, A novel method for fabricating an electrospun poly(vinyl alcohol)/cellulose nanocrystals composite nanofibrous filter with low air resistance for high-efficiency filtration of particulate matter, ACS Sustain. Chem. Eng. 7 (2019) 8706–8714.
[19] S. Wang, X. Zhao, X. Yin, J. Yu, B. Ding, Electret polyvinylidene fluoride nanofibers hybridized by polytetrafluoroethylene nanoparticles for high-efficiency air filtration, ACS Appl. Mater. Interfaces 8 (2016) 23985–23994.
[20] R. Balgis, H. Murata, Y. Goi, T. Ogi, K. Okuyama, L. Bao, Synthesis of dual-size cellulose-polyvinylpyrrolidone nanofiber composites via one-step electrospinning method for high-performance air filter, Langmuir 33 (2017) 6127–6134.
[21] J. Li, D. Zhang, T. Yang, S. Yang, X. Yang, H. Zhu, Nanofibrous membrane of graphene oxide-in-polyacrylonitrile composite with low filtration resistance for the effective capture of PM2.5, J. Membr. Sci. 551 (2018) 85–92.
[22] P. Zhang, D. Wan, Z. Zhang, G. Wang, J. Hu, G. Shao, RGO-functionalized polymer nanofibrous membrane with exceptional surface activity and ultra-low airflow resistance for PM2.5 filtration, Environ. Sci. Nano 5 (2018) 1813–1820.
[23] S.F. Dehghan, F. Golbabaei, B. Maddah, M. Latifi, H. Pezeshk, M. Hasanzadeh, F. Akbar-Khanzadeh, Optimization of electrospinning parameters for polyacrylonitrile-MgO nanofibers applied in air filtration, J. Air Waste Manage. Assoc. 66 (2016) 912–921.
[24] Y. Zhang, S. Yuan, X. Feng, H. Li, J. Zhou, B. Wang, Preparation of nanofibrous metal-organic framework filters for efficient air pollution control, J. Am. Chem. Soc. 138 (2016) 5785–5788.
[25] N. Wang, Y. Si, N. Wang, G. Sun, M. El-Newehy, S.S. Al-Deyab, B. Ding, Multilevel structured polyacrylonitrile/silica nanofibrous membranes for high-performance air filtration, Sep. Purif. Technol. 126 (2014) 44–51.
[26] Y. Yang, S. Zhang, X. Zhao, J. Yu, B. Ding, Sandwich structured polyamide-6/polyacrylonitrile nanonets/bead-on-string composite membrane for effective air filtration, Sep. Purif. Technol. 152 (2015) 14–22.
[27] A. Nicosia, W. Gieparda, J. Foksowicz-Flaczyk, J. Walentowska, D. Wesołek, B. Vazquez, F. Prodi, F. Belosi, Air filtration and antimicrobial capabilities of electrospun PLA/PHB containing ionic liquid, Sep. Purif. Technol. 154 (2015) 154–160.
[28] Z. Wang, C. Zhao, Z. Pan, Porous bead-on-string poly(lactic acid) fibrous membranes for air filtration, J. Colloid Interface Sci. 441 (2015) 121–129.
[29] N. Wang, A. Raza, Y. Si, J. Yu, G. Sun, B. Ding, Tortuously structured polyvinyl chloride/polyurethane fibrous membranes for high-efficiency fine particulate filtration, J. Colloid Interface Sci. 398 (2013) 240–246.
[30] F. Zuo, S. Zhang, H. Liu, H. Fong, X. Yin, J. Yu, B. Ding, Free-standing polyurethane nanofiber/nets air filters for effective PM capture, Small 13 (2017) 1702139.
[31] J. Choi, B.J. Yang, G.N. Bae, J.H. Jung, Herbal extract incorporated nanofiber fabricated by an electrospinning technique and its application to antimicrobial air filtration, ACS Appl Mater Interfaces 7 (2015) 25313–25320.
[32] M. Li, Y. Feng, K. Wang, W.F. Yong, L. Yu, T.S. Chung, Novel hollow fiber air filters for the removal of ultrafine particles in PM2.5 with repetitive usage capability, Environ. Sci. Technol. 51 (2017) 10041–10049.
[33] J. Nemoto, T. Saito, A. Isogai, Simple freeze-drying procedure for producing nanocellulose aerogel-containing, high-performance air filters, ACS Appl Mater Interfaces 7 (2015) 19809–19815.
[34] X. Fan, Y. Wang, L. Kong, X. Fu, M. Zheng, T. Liu, W.-H. Zhong, S. Pan, A nanoprotein-functionalized hierarchical composite air filter, ACS Sustain. Chem. Eng. 6 (2018) 11606–11613.
[35] Y. Liao, C.-H. Loh, M. Tian, R. Wang, A.G. Fane, Progress in electrospun polymeric nanofibrous membranes for water treatment: Fabrication, modification and applications, Prog. Polym. Sci. 77 (2018) 69–94.
[36] G. Yang, X. Li, Y. He, J. Ma, G. Ni, S. Zhou, From nano to micro to macro: Electrospun hierarchically structured polymeric fibers for biomedical applications, Prog. Polym. Sci. 81 (2018) 80–113.
[37] Y. Liao, R. Wang, M. Tian, C. Qiu, A.G. Fane, Fabrication of polyvinylidene fluoride (PVDF) nanofiber membranes by electro-spinning for direct contact membrane distillation, J. Membr. Sci. 425–426 (2013) 30–39.
[38] R.H. Colby, L.J. Fetters, W.G. Funk, W.W. Graessley, Effects of concentration and thermodynamic interaction on the viscoelastic properties of polymer solutions, Macromolecules 24 (1991) 3873–3882.
[39] C.J. Cooper, A.K. Mohanty, M. Misra, Electrospinning process and structure relationship of biobased poly(butylene succinate) for nanoporous fibers, ACS Omega 3 (2018) 5547–5557.
[40] C.J. Thompson, G.G. Chase, A.L. Yarin, D.H. Reneker, Effects of parameters on nanofiber diameter determined from electrospinning model, Polymer 48 (2007) 6913–6922.
[41] J. Xue, T. Wu, Y. Dai, Y. Xia, Electrospinning and electrospun nanofibers: methods, materials, and applications, Chem. Rev. 119 (2019) 5298–5415.
[42] S. De Vrieze, T. Van Camp, A. Nelvig, B. Hagström, P. Westbroek, K. De Clerck, The effect of temperature and humidity on electrospinning, J. Mater. Sci. 44 (2009) 1357–1362.
[43] C.L. Casper, J.S. Stephens, N.G. Tassi, D.B. Chase, J.F. Rabolt, Controlling surface morphology of electrospun polystyrene fibers: effect of humidity and molecular weight in the electrospinning process, Macromolecules 37 (2004) 573–578.
[44] L. Huang, N.-N. Bui, S.S. Manickam, J.R. McCutcheon, Controlling electrospun nanofiber morphology and mechanical properties using humidity, J. Polym. Sci., Part B: Polym. Phys. 49 (2011) 1734–1744.
[45] E.S. Medeiros, L.H.C. Mattoso, R.D. Offeman, D.F. Wood, W.J. Orts, Effect of relative humidity on the morphology of electrospun polymer fibers, Can. J. Chem. 86 (2008) 590–599.
[46] Y. Wang, W. Li, Y. Xia, X. Jiao, D. Chen, Electrospun flexible self-standing γ-alumina fibrous membranes and their potential as high efficiency fine particulate filtration media, J. Mater. Chem. A 2 (2014) 15124–15131.
[47] R. Mostofi, A. Noël, F. Haghighat, A. Bahloul, J. Lara, Y. Cloutier, Impact of two particle measurement techniques on the determination of N95 class respirator filtration performance against ultrafine particles, J. Hazard. Mater. 217–218 (2012) 51–57.
[48] C.H. Jung, H.-S. Park, Y.P. Kim, Theoretical study for the most penetrating particle size of dust-loaded fiber filters, Sep. Purif. Technol. 116 (2013) 248–252.
[49] A. Podgórski, A. Bałazy, L. Gradoń, Application of nanofibers to improve the filtration efficiency of the most penetrating aerosol particles in fibrous filters, Chem. Eng. Sci. 61 (2006) 6804–6815.
[50] N. Wang, Z. Zhu, J. Sheng, S.S. Al-Deyab, J. Yu, B. Ding, Superamphiphobic nanofibrous membranes for effective filtration of fine particles, J. Colloid Interface Sci. 428 (2014) 41–48.
[51] J.H. Vincent, Air filtration: An integrated approach to the theory and applications of fibrous filters: R. C. Brown, Pergamon Press, Oxford, 1993.
[52] C.N. Davies, The Separation of Airborne Dust and Particles, 1952.
[53] R.M. Werner, L.A. Clarenburg, Aerosol filters pressure drop across single-component glass fiber filters, Indus. Eng. Chem. Process Design Dev. 4 (1965) 288–293.
[54] X. Fan, Y. Wang, W.H. Zhong, S. Pan, Hierarchically structured all-biomass air filters with high filtration efficiency and low air pressure drop based on pickering emulsion, ACS Appl Mater Interfaces 11 (2019) 14266–14274.
[55] H. Souzandeh, K.S. Johnson, Y. Wang, K. Bhamidipaty, W.H. Zhong, Soy-protein-based nanofabrics for highly efficient and multifunctional air filtration, ACS Appl Mater Interfaces 8 (2016) 20023–20031.
[56] Z. Zhong, Z. Xu, T. Sheng, J. Yao, W. Xing, Y. Wang, Unusual air filters with ultrahigh efficiency and antibacterial functionality enabled by ZnO nanorods, ACS Appl Mater Interfaces 7 (2015) 21538–21544.
[57] R. Al-Attabi, L.F. Dumée, L. Kong, J.A. Schütz, Y. Morsi, High efficiency poly(acrylonitrile) electrospun nanofiber membranes for airborne nanomaterials filtration, Adv. Eng. Mater. 20 (2018) 1700572.
[58] Y. Bai, C.B. Han, C. He, G.Q. Gu, J.H. Nie, J.J. Shao, T.X. Xiao, C.R. Deng, Z.L. Wang, Washable multilayer triboelectric air filter for efficient particulate matter PM2.5 removal, Adv. Funct. Mater. 28 (2018) 1706680.
[59] V. Kadam, Y.B. Truong, C. Easton, S. Mukherjee, L. Wang, R. Padhye, I.L. Kyratzis, Electrospun polyacrylonitrile/β-cyclodextrin composite membranes for simultaneous air filtration and adsorption of volatile organic compounds, ACS Appl. Nano Mater. 1 (2018) 4268–4277.
[60] C. Wang, S. Wu, M. Jian, J. Xie, L. Xu, X. Yang, Q. Zheng, Y. Zhang, Silk nanofibers as high efficient and lightweight air filter, Nano Research 9 (2016) 2590–2597.
[61] J. Wang, W. Zhao, B. Wang, G. Pei, C. Li, Multilevel-layer-structured polyamide 6/poly(trimethylene terephthalate) nanofibrous membranes for low-pressure air filtration, J. Appl. Polym. Sci. 134 (2017).
[62] Z. Zeng, X.Y.D. Ma, Y. Zhang, Z. Wang, B.F. Ng, M.P. Wan, X. Lu, Robust lignin-based aerogel filters: high-efficiency capture of ultrafine airborne particulates and the mechanism, ACS Sustain. Chem. Eng. 7 (2019) 6959–6968.
[63] X. Zhao, Y. Li, T. Hua, P. Jiang, X. Yin, J. Yu, B. Ding, Low-resistance dual-purpose air filter releasing negative ions and effectively capturing PM2.5, ACS Appl Mater Interfaces 9 (2017) 12054–12063.